CHEMBIOCHEM

DOI: 10.1002/cbic.201100116

Revisiting the Mechanism of the Triosephosphate Isomerase Reaction: The Role of the Fully Conserved Glutamic Acid 97 Residue

Moumita Samanta,[a] M. R. N. Murthy,[a] Hemalatha Balaram,[b] and Padmanabhan Balaram*[a]

An analysis of 503 available triosephosphate isomerase sequences revealed nine fully conserved residues. Of these, four residues—K12, H95, E97 and E165—are capable of proton transfer and are all arrayed around the dihydroxyacetone phosphate substrate in the three-dimensional structure. Specific roles have been assigned to the residues K12, H95 and E165, but the nature of the involvement of E97 has not been established. Kinetic and structural characterization is reported for the E97Q and E97D mutants of *Plasmodium falciparum* triosephosphate isomerase (*Pf* TIM). A 4000-fold reduction in k_{cat} is observed for E97Q, whereas the E97D mutant shows a 100-fold reduction. The control mutant, E165A, which lacks the key catalytic base, shows an approximately 9000-fold drop in activity. The integrity of the overall fold and stability of the dimeric structure have been demonstrated by biophysical studies. Crystal structures of E97Q and E97D mutants have been determined at 2.0 Å resolution. In the case of the isosteric replacement of glutamic acid by glutamine in the E97Q mutant a large conformational change for the critical K12 side chain is observed, corresponding to a *trans*-to-*gauche* transition about the Cγ–Cδ (χ^3) bond. In the E97D mutant, the K12 side chain maintains the wild-type orientation, but the hydrogen bond between K12 and D97 is lost. The results are interpreted as a direct role for E97 in the catalytic proton transfer cycle. The proposed mechanism eliminates the need to invoke the formation of the energetically unfavourable imidazolate anion at H95, a key feature of the classical mechanism.

Introduction

The selective pressure of molecular evolution is expected to result in the conservation of key amino acid residues and three-dimensional structural features that are critical for biochemical function. Enzymes from diverse organisms, but which catalyse the same chemical reaction, can have substantially different sequences, with relatively small numbers of completely conserved residues, when large datasets are aligned. The relationship between three-dimensional structure and catalytic function in enzymes is often obscured by the complexities of the three-dimensional structure. Karplus and Kuriyan noted that "The engineering principles underlying protein design are truly baroque, with evolutionary tinkering resulting in molecular machines that may be effective and efficient but whose three-dimensional structures are often so complicated as to obscure the mechanism of action".[1]

Triosephosphate isomerase (TIM) is a ubiquitous enzyme controlling the central step in glycolysis, catalysing the isomerization of dihydroxyacetone phosphate (DHAP) and glyceraldehyde-3-phosphate (GAP).[2,3] The isomerization involves proton transfer between adjacent carbon atoms of the substrate and the reaction proceeds at a rate limited only by diffusion.[4] The classic studies of Rose and Knowles on TIM are central to the historical development of mechanistic enzymology.[5–7] In reviewing a long line of incisive studies,[6,7] Knowles characterized TIM as an enzyme fashioned by "evolution to perfection".[8] Clearly, random mutations and phenotypic selection have designed an enzyme active site that has reached the limits of catalytic efficiency.[9]

The availability of a growing dataset of TIM sequences and three-dimensional structures from diverse organisms prompted us to revisit some outstanding issues relating to the mechanism of the isomerization reaction. Three residues—K12, H95 and E165—have been established as critical residues in binding and catalysis.[10–14] Curiously, the small polar substrates DHAP and GAP are anchored to the protein surface through hydrogen-bonding interactions involving the backbone NH groups of S211, G232, G233 and G171, with the positively charged ε-amino group of K12 providing the only obvious electrostatic interaction, being located at a distance of 3.13 Å (PDB ID: 1NEY)[15] from the oxygen atom bonded to C3 of the substrate. This observation led Knowles (1991) to quote Pauling (1960),[16] who suggested that "a main chain –NH– bond is worth about half a charge", suggesting that interaction with the neutral backbone "effectively balances the dianionic charge of the phospho group".[2] The phosphate binding energy has been linked to the transition state stabilization that

[a] *M. Samanta, M. R. N. Murthy, Prof. P. Balaram*
Molecular Biophysics Unit, Indian Institute of Science
Bangalore-560012 (India)
E-mail: pb@mbu.iisc.ernet.in

[b] *H. Balaram*
Molecular Biology and Genetics Unit
Jawaharlal Nehru Centre for Advanced Scientific Research
Bangalore-560064 (India)

Supporting information for this article is available on the WWW under http://dx.doi.org/10.1002/cbic.201100116.

leads to the large observed catalytic rate enhancement.[17,18] A critical role for K12 was established by the early work of Knowles, which demonstrated that mutation of this residue resulted in a dramatic loss in activity.[12] Subsequent theoretical work points to the key role for K12 in transition state stabilization.[19] More recently, Richard has elegantly demonstrated that the cationic side chain of K12 stabilizes the transition state by as much as 7.8 kcal mol^{-1}.[13] By a two-part substrate approach, it has been demonstrated that the contribution of K12 to the transition state stabilization is 6.3 kcal mol^{-1} greater than that provided by the ammonium ion in the K12G mutant.[20] This study establishes that precise orientation and tethering of the alkyl ammonium side chain of K12 is central to the catalytic rate enhancement. Go et al. (2010) have more recently pointed out that "the phosphate gripper motif of TIM is unlikely to contribute any significant enthalphic advantage, but will be effective in an entropic sense by liberating waters of hydration".[13] The carboxylate of E165 acts as a base initiating the first step of proton abstraction from the substrate and completes the catalytic cycle by retransfer of the proton to form the isomerized product. H95 mediates the proton transfer.

The careful experimental work of Knowles' group led to the conclusion that the neutral imidazole side chain of H95 functions as an electrophile in the catalytic process.[21] This unusual situation would require the formation of an *imidazolate* anion, a process characterized by a very high pK_a value ($\approx$14). Combined QM/MM calculations carried out by Bash and Karplus lent support to this unusual mechanism,[19] which, as Knowles acknowledges, "runs counter to the prejudices of mechanistic chemistry".[21] The availability of a high-resolution crystal structure of an enzyme/substrate complex (yeast TIM/DHAP complex) (PDB ID: 1NEY),[15] together with the growing volume of sequences and related three-dimensional structures, prompted us to re-examine the distribution of the fully conserved residues in the vicinity of the enzyme active site. Inspection of a dataset of 503 TIM sequences, from diverse organisms of archaeal, bacterial and eukaryotic origins, reveals only nine fully conserved residues: K12, T75, H95, E97, C126, E165, P166, G209 and G228 (for all the fully conserved residues, the numbering schemes are identical for both *Pf* and yeast triosephosphate isomerase). Of these, E97 is positioned directly at the active site in close proximity to K12 and H95 as shown in Figure 1. The presence of an ionizable side chain strategically positioned between K12 and H95 suggests a potential role in the proton transfer reaction.

Nearly twenty years ago, Knowles and co-workers reported that a single-residue mutant, E97D, retained full catalytic activity,[22] an observation that suggests no direct role for E97 in catalysis, despite its proximity to the active site and its complete conservation. Intrigued by this observation, we have generated and characterized, structurally and kinetically, the active site mutants E97Q and E97D in *Plasmodium falciparum* triosephosphate isomerase (*Pf* TIM). The E97Q mutant, in which the ionizable glutamic acid side chain is replaced by the isosteric, non-ionizable glutamine side chain, is almost completely inactive. The aspartic acid replacement results in side chain shortening in the E97D mutant, which displays significantly attenuated catalytic activity. Crystal structure determination of both mutants has provided insights into the role of residue 97 and established the dramatic reorientation of the critical K12 side chain in the E97Q mutant.

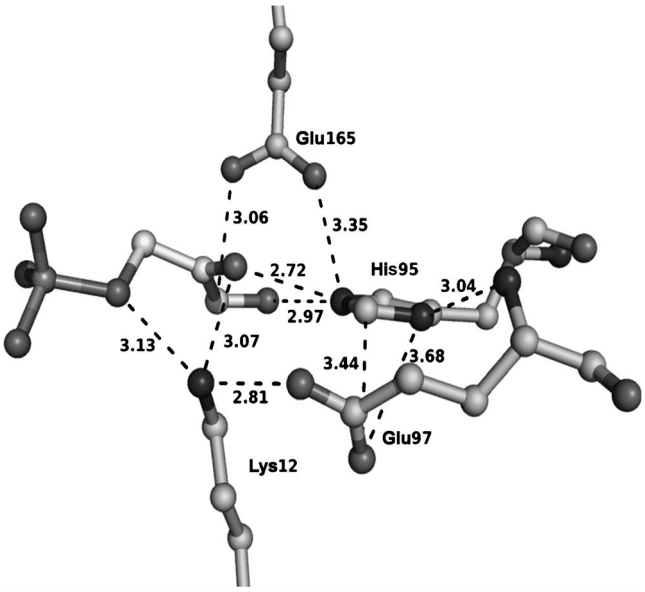

Figure 1. View of the glutamic acid 97 (E97) residue along with the active site residues K12, H95 and E165 with DHAP bound at the active site in the yeast TIM/DHAP complex structure (PDB ID: 1NEY). All figures were generated with Pymol (http://www.pymol.org).

Results

Characterization of mutants

The protein mutants were characterized by mass spectrometry and by determination of their crystal structures. Although the presence of each mutation was confirmed by sequencing of the cloned gene, it was felt that an unambiguous characterization of the mutation in the protein was both desirable and important, in view of the differences between our results on the E97D mutant and the results of Knowles and co-workers on the corresponding mutant of the chicken enzyme.[22] The details of the ESI MS characterization are presented in Figure S1 in the Supporting Information.

The availability of single crystals facilitated further characterization. Figure 2 A and B provide a view of the electron density in the vicinity of the site of the mutations. In the E97D mutant, characterization of the mutation is readily accomplished by fitting the observed electron density, as a result of the shortening of the side chain. In contrast, the electron density does not permit any distinction between the glutamic acid and the glutamine side chains. In the case of the E97Q mutant, a dramatic reorientation of the proximal K12 side chain is observed. This is presumably a consequence of the loss of the favourable interaction between the positively charged ε-amino group and the negatively charged carboxylate as a result of the E97Q mutation. This is further elaborated in the Discussion section.

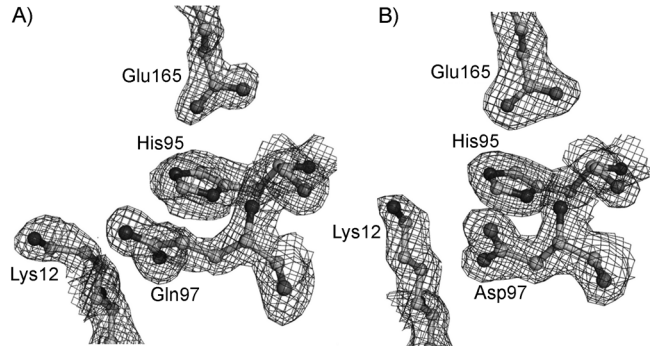

Figure 2. Electron-density maps ($2|F_o-F_c|$ contoured at 1.0σ) at the active site residues and residue 97 in: A) E97Q (3PSW), and B) E97D (3PSV) structures.

Enzyme activity

A comparison of the activities of the mutants and the wild-type enzyme as a function of substrate concentration is shown in Figure S2. Table 1 summarizes the kinetic parameters determined for the *Pf* TIM WT and the three mutants E97Q, E97D and E165A. The E97Q and the E165A mutants exhibit approximately 4000- to 9000-fold drops in k_{cat}, suggesting the almost complete abolition of catalytic activity upon mutation. The E97D mutant shows an appreciably higher k_{cat} value, albeit still 100 times lower than that of the native enzyme. The background activities of the host AA200 cells and the host cells transformed with the vector (pTrc99A) were also measured. The observed background specific activity of 0.001 $\mu mol\,s^{-1}\,mg^{-1}$ may be compared with those obtained for the *Pf* TIM WT (108 $\mu mol\,s^{-1}\,mg^{-1}$), E97Q (0.046 $\mu mol\,s^{-1}\,mg^{-1}$) and E97D (1.6 $\mu mol\,s^{-1}\,mg^{-1}$). These results suggests that the shortening of the acidic side chain at position 97 in the E97D mutant results in a significant reduction (100-fold) in activity. Nevertheless an appreciable level of isomerase activity is still observable. In contrast, the reduction in activity of the E97Q mutant is $\approx$4000-fold whereas that observed for the E165A mutant, which lacks the catalytic group involved in the initial proton abstraction step, is $\approx$9000-fold. The replacement of the glutamic acid at position 97 by glutamine can result only in changes in electrostatic and hydrogen-bonding interactions, because the two residues are almost identical in shape and size, differing only in the ionizabilities of the side chains. The TIM active site is located close to the dimer interface, although all the residues important for the chemical steps of catalysis are located on a single subunit. The side chain of residue 97 does indeed make hydrogen bond contacts to the fully conserved T75 residue from the other subunit (see the Discussion). We therefore examined the concentration dependence of activity for the wild-type enzyme and for the E97Q and E97D mutants over a wide protein concentration range of 0.2 μM to 4 μM. Figure S3 shows that over this concentration regime there is no change in the specific activities of the wild-type and mutant enzymes, suggesting that the replacements at residue 97 have not significantly altered the stability of the dimer. It might be noted that monomeric TIMs engineered by Wierenga's group retain the overall $(\alpha/\beta)_8$ barrel fold, but display an approximately 1000-fold fall in activity, suggesting a complete dependence of catalytic efficiency on dimer integrity.[23]

Table 1. Kinetic parameters for the wild-type enzyme and for the mutants E97Q, E97D and E165A.

Enzymes	k_{cat} [s^{-1}]	K_m [mM]	k_{cat}/K_m [$mM^{-1}\,s^{-1}$]
wild-type	$4.30\pm0.03\times10^3$	0.35 ± 0.05	1.22×10^4
E97Q	1.00 ± 0.15	1.20 ± 0.20	0.90
E97D	$4.20\pm0.80\times10$	0.50 ± 0.02	8.40×10
E165A	0.45 ± 0.08	0.43 ± 0.05	0.93

Biophysical studies

Figure S4 shows the far-UV CD and fluorescence emission spectra of the wild-type enzyme and of the mutants E97Q and E97D. The identical natures of the spectra suggest that the overall fold and the tryptophan residue (W11 and W168) environments are largely unperturbed by site-specific mutations at position 97. Furthermore, the thermal melting profiles determined by monitoring of CD ellipticity at 222 nm are almost identical for the three proteins. The positions of the fluorescence maxima (331 nm)[24] were identical for the three proteins and were concentration-independent over the concentration range from 0.5 to 20 μM (Figure S5). Analytical gel filtration profiles (Figure S6), determined over a protein concentration range from 0.5 to 20 μM, reveal identical elution volumes for the wild-type enzyme and for the E97Q and E97D mutants, confirming the dimeric nature of all three proteins, even at the lowest concentration studied.

Analysis of the crystal structures

Crystals of the *Pf* TIM mutants E97Q and E97D each diffracted to 2.0 Å, with one protein dimer in the asymmetric unit. In both cases, loop 6 was in the "open" conformation and the active site was unliganded. In the liganded, loop-closed conformation of TIM, the flexible loop 6 serves to sequester the reactive enediol intermediate and to expel water molecules from the immediate vicinity of the reactive functionalities.[9,31,32] Despite attempts to crystallize the mutants in the presence of ligands, none of the crystals examined incorporated the ligand. In each of the mutants, electron density corresponding to an ethylene glycol molecule and a sulfate ion could be clearly visualized. Figure 3 compares the active site structure of unliganded *Pf* TIM in the loop 6 open conformation (PDB ID: 1YDV)[25] with the corresponding residues in the two mutant forms. In the case of *Pf* TIM, and indeed TIMs from other sources, ligand binding and loop 6 closure leaves the K12, E97 and H95 residues unchanged, with a small movement of the E165 residue. Inspection of Figure 3B immediately reveals a large conformational change involving the K12 side chain in the case of the E97Q mutant. In all TIM structures determined so far, the K12 side chain adopts a fully extended conformation.

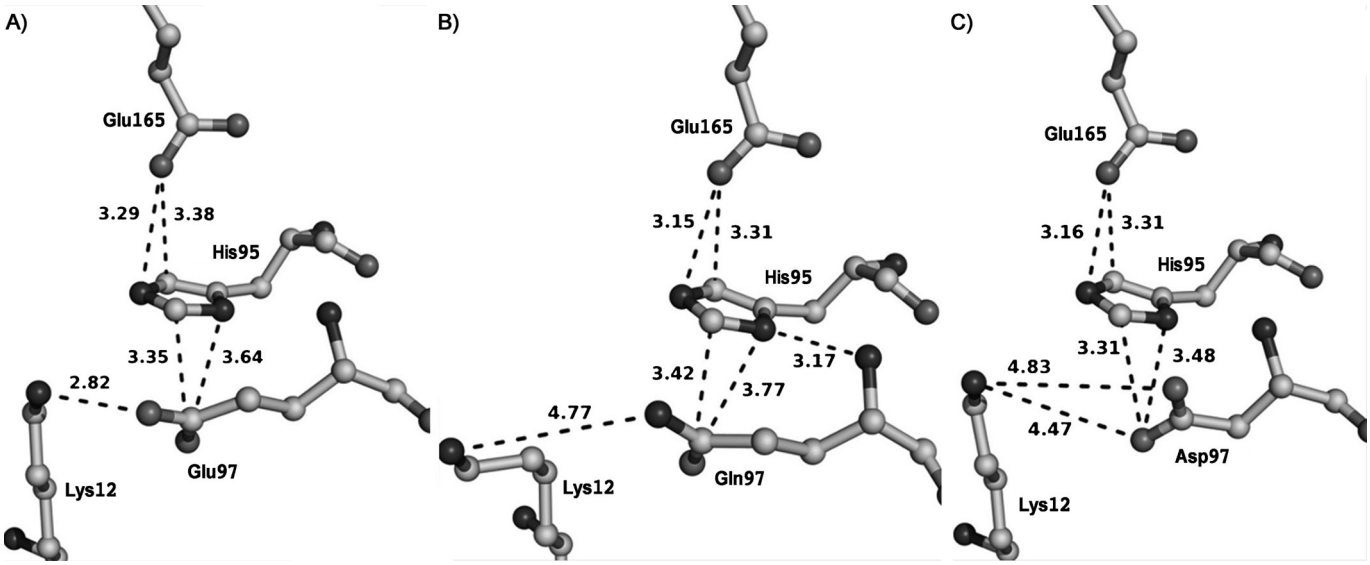

Figure 3. Comparative views of the active site residues and the key interacting distances in: A) the *Pf* TIM wild type (PDB ID: 1YDV), B) E97Q (PDB ID: 3PSW), and C) E97D (PDB ID: 3PSV).

In contrast, in the E97Q structure, the dihedral angle $\chi 3$ (Cγ–Cδ) has a *gauche*(−) conformation ($\chi 3 = -75.1^{\circ}$). In all other structures, $\chi 3$ has a *trans* conformation ($\chi 3 \approx 180^{\circ}$). Both in the yeast TIM/DHAP complex (PDB ID: 1NEY)[15] and in the unliganded *Pf* TIM WT structure (PDB ID: 1YDV)[25] the ε-amino group of K12 forms a hydrogen bond with the carboxylic acid side chain of E97. The observed N–O distances are 2.81 Å in the yeast/DHAP complex and 2.82 Å in the unliganded *Pf* TIM wild type. In the E97Q mutant, the conformational change in the lysine side chain results in a loss of the hydrogen-bonding interaction; the observed N–O distance increases to 4.8 Å.

In the case of the E97D mutant, the K12 side chain adopts the fully extended conformation observed in all other TIM structures. The shortening of the side chain at position 97 from Glu to Asp results in a loss of the hydrogen-bonding interaction between the carboxylic acid group at position 97 and the amino group at position 12. In this case a N–O distance of 4.8 Å is observed.

Mutation of the fully conserved Glu(E)97 residue of *Pf* TIM to Gln (Q) results in a dramatic reduction in isomerase activity. The carboxamide group of the glutamine side chain is isosteric with the carboxylic acid moiety of the glutamic acid side chain. They differ, however, in an important respect in their hydrogen-bonding abilities. Figure 4 compares the hydrogen bonds formed by the residue 97 side chain in the *Pf* TIM wild type and in the E97Q and E97D structures. In the native enzyme, the carboxylic acid group of E97 is involved in multiple hydrogen-bonding interactions. One oxygen atom participates in three potential hydrogen-bonding interactions with residues from the other subunit. Three short inter-subunit interactions can be identified: with the Thr75 side chain hydroxy group (O–O: 2.6 Å), the Thr75 backbone NH (N–O: 3.06 Å) and the

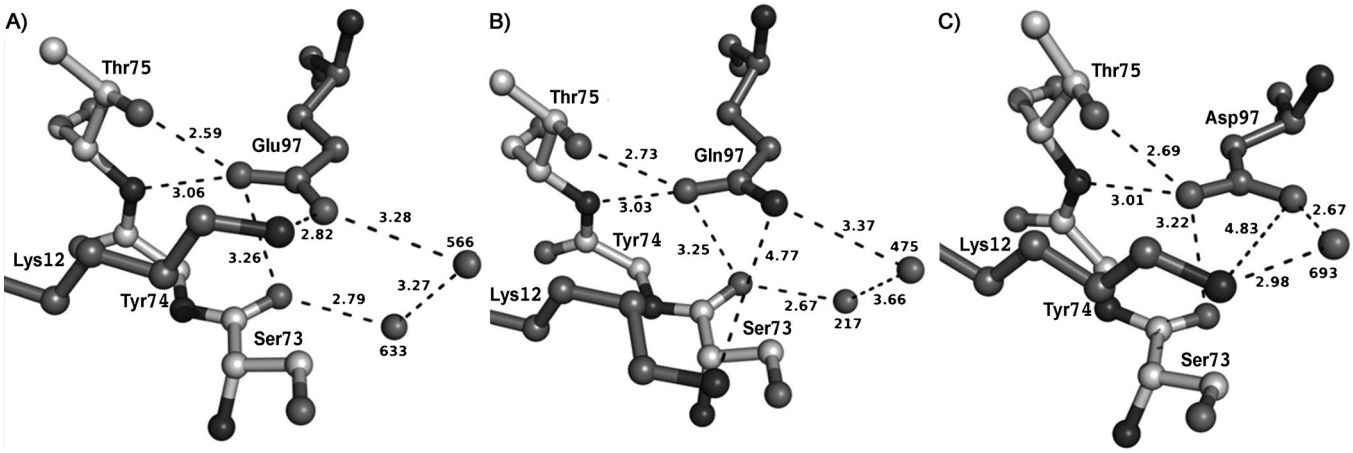

Figure 4. Hydrogen-bonding interactions involving the residue 97 side chain with surrounding residues and water molecules: A) in the unliganded *Pf* TIM wild type (PDB ID: 1YDV), and B) in E97Q (PDB ID: 3PSW), and C) in E97D (PDB ID: 3PSV). Dark grey and light grey represent residues from different subunits.

Ser73 backbone CO (O–O: 3.26 Å). Although the state of ionization of the carboxylic acid group cannot be directly ascertained through the location of the H atom, the observation of a rather short O–O distance between the Ser73 backbone CO group and the Glu97 side chain oxygen is suggestive of—but does not definitively establish—an un-ionized carboxylic acid group at this position. This is consistent with the participation of the oxygen in three hydrogen-bonding interactions, acting as a donor in one case and an acceptor in the other two. The second side chain oxygen atom of Glu97 makes a hydrogen bond to the ε-amino group of Lys12 and a water molecule (W566), which in turn is hydrogen-bonded to the water molecule W633, which also interacts with the S73 backbone carbonyl group. These two water molecules are conserved in all TIM structures from diverse organisms, with the exceptions of the tetrameric enzymes from the thermophilic organisms *Methanocaldococcus janaschii* (PDB ID: 2H6R)[26] and *Pyrococcus woesei* (PDB ID: 1HG3).[27] In the E97Q mutant, the hydrogen-bonding interactions across the dimer interface are maintained. The large conformational change in the K12 side chain presumably arises as a result of the close proximity of the amide NH_2 of Q97 and the ε-NH_2 of K12. It should be noted that in fitting of *primary* amide side chains to electron densities, distinctions between the two possible orientations of the amide group are generally made, by inspection of the potential hydrogen-bonding interactions and steric clashes.[28] In the liganded TIM structures, a conserved water molecule forms a hydrogen-bonded bridge between the lysine ε-NH_2 group and one of the phosphate oxygen atoms. This is demonstrated in the case of the *Pf* TIM wild type/3PG complex (PDB ID: 2VFI) shown in Figure 5A, in which W2167 acts as the bridge. In the unliganded TIM structures, several water molecules form a hydrogen-bonded cluster at the unoccupied active site (Figure 6). Ligand binding results in a displacement of these water molecules. In the E97Q structure, displacement of the Lys ε-amino group from the position occupied in the wild-type enzyme places it in the position of the bridging water molecule, resulting in the formation of a hydrogen bond to one of the oxygen atoms of the sulfate anion, located near the active site (Figure 5B). Interestingly, in the E97D structure, in which K12 occupies a position identical to that in the wild-type enzyme, the bridging water molecule (W431) forms a hydrogen bond to the Lys ε-amino group and the sulfate ion (Figure 5C). The identical orientation of the K12 side chain in the wild-type and the E97D structures suggests that the hydrogen-bonding interaction between the ε-ammonium group and the residue 97 carboxylate group is not critical for positioning the catalytically crucial K12 side chain. The absence of any effect of the E97Q mutation on the stability of the dimer is established by the absence of concentration dependence of enzyme activity, spectroscopic properties and the elution volumes in analytical gel filtration experiments. This is consistent with the crystallographic observations, which reveal no change in interactions involving this residue across the subunit interface. The dramatic loss in activity is also consistent with structural evidence, which shows a large change in the position of the critical ε-amino group of K12. Previous work has established that mutation of the K12 residue results in almost complete loss of activity. Lodi et al. (1994) reported k_{cat} values of 0.018 s^{-1} for K12M, 48 s^{-1} for K12R, 6.3 s^{-1} for K12H (pH 6.1) and 0.89 s^{-1} for K12H (pH 7.5). The corresponding yeast wild-type enzyme has a k_{cat} value of 8700 s^{-1}.[12] More recently, Go et al. have reported a k_{cat} value of 0.6 s^{-1} for the K12G mutant of TIM.[13] These results suggest that precise orientation of the K12 residue is essential for optimal activity of the enzyme. Furthermore, the unchanged K12 orientation, together with impaired activity in the E97D mutant, points to a direct role for the E97 carboxylate in the catalytic process. The hydrogen bond between E97 and K12 side chains, both of which are completely conserved, is also suggestive of an important role for this ionizable side chain in the proton-transfer reaction.

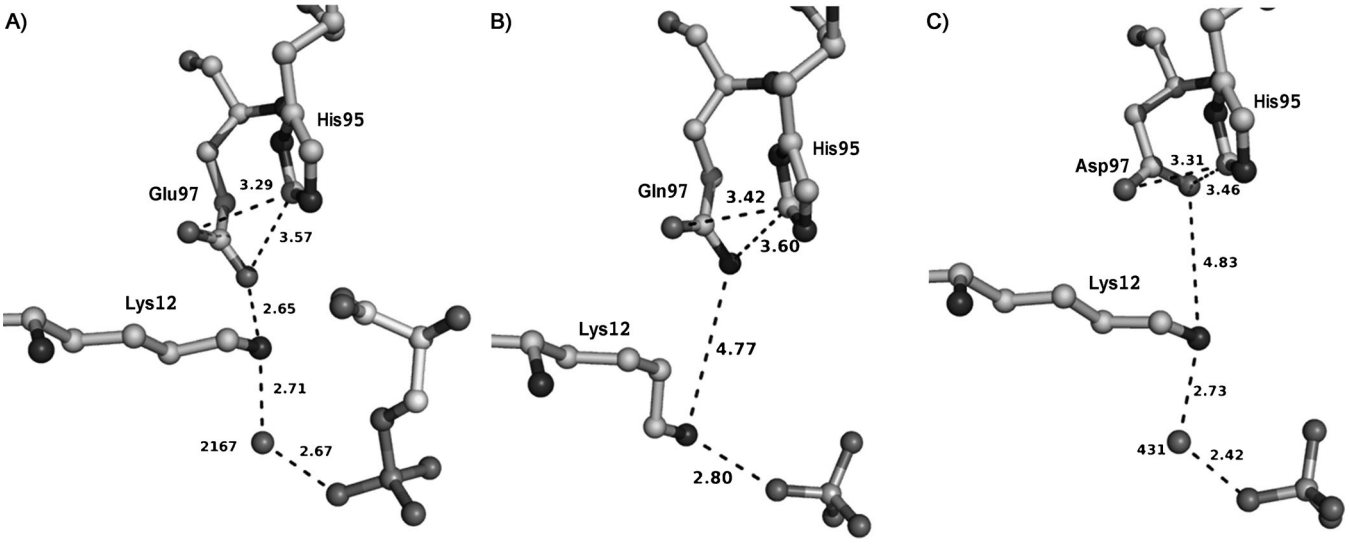

Figure 5. Important interactions of the critical residue K12 side chain: A) in the *Pf* TIM/3PG structure (PDB ID: 2VFI), and B) in E97Q (PDB ID: 3PSW), and C) in E97D (PDB ID: 3PSV).

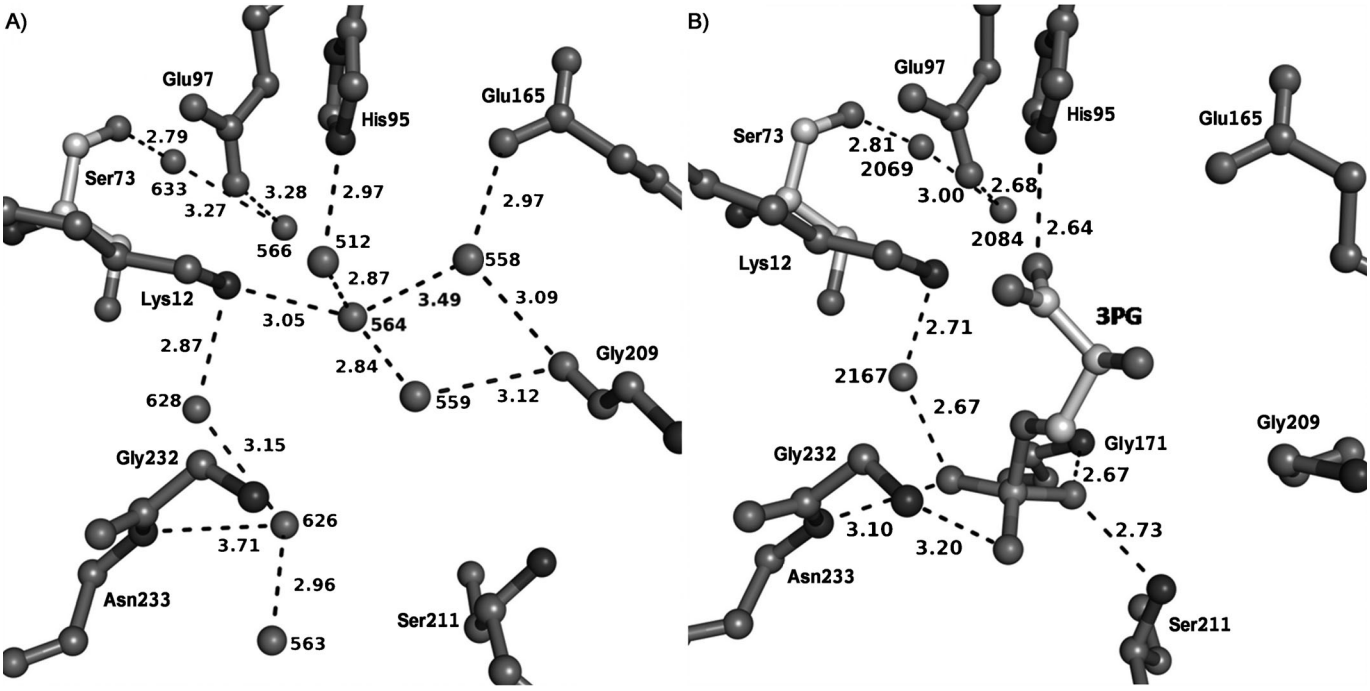

Figure 6. Water network at the active site of TIM: A) when unliganded (PDB ID: 1YDV), and B) liganded (3PG, PDB ID: 2VFI). Dark grey and light grey represent residues from different subunits.

Discussion

Revisiting the proton transfer mechanism in TIM

The stereospecific abstraction of the *pro-R* hydrogen from the hydroxymethylene group of DHAP by the carboxylate of E165 and the subsequent formation of the enediolate intermediate constitutes the initial, critical step in the isomerization reaction.[5] The K12 ε-amino group is well positioned to provide electrostatic stabilization of the enediolate intermediate, a common feature of the aldose-ketose isomerases, as pointed out by Rose nearly half a century ago.[5,29] His95 is the other key residue directly involved in facilitating the proton-transfer process. The extensive work of Knowles and his collaborators has established an important attribute of H95: namely that the imidazole side chain is neutral (uncharged).[21] Inspection of the crystal structures of TIMs from different sources establishes that the positions of the side chains of the Lys12, His95 and Glu97 residues are identical, and remain unchanged both in loop 6 open, unliganded structures and in loop 6 closed, liganded structures. This suggests a largely preexisting orientation of these three active-site residues. Substrate binding and loop closure results only in the movement of the catalytically critical E165 side chain.[14,30] Loop 6 dynamics are of central importance in the TIM reaction.[31] Loop closure over the bound substrate serves to dehydrate the active site and to position the hinge residue E165 for the proton-abstraction step. The placement of this side chain in a "hydrophobic cage" has been suggested to be responsible for an increase in the basicity of the E165 carboxylate group.[32] The work of Knowles and coworkers led to the suggestion that H95 functions as an electrophile, donating a proton from its neutral state, resulting in the formation of an imidazolate anion, which then reabstracts a proton from the C1 position of the enediol, with subsequent reprotonation of the substrate by the carboxylic acid at E165.[11] Lodi and Knowles argued that the neutral state of His95 is a consequence of its position at the positive end of the macrodipole produced by the α helix formed over the residues 97–102.[33] The formation of an imidazolate anion is, however, a process that is not really anticipated on the basis of the estimated acidity of neutral imidazole ($pK_a \approx 14$). In an influential overview, Knowles raised a question: "Why, when everything else about this enzyme seems chemically so reasonable, it should fail to use the more powerful electrophile [imidazolium ion of protonated His95], remains a puzzle."[9] Nevertheless, this proposal has been completely accepted, with support being derived from combined QM/MM calculations carried out by Karplus and co-workers.[19,34] Furthermore, FTIR investigations have established that in enzyme/substrate complexes, the carbonyl stretching frequency of DHAP is sensitive to mutations of H95 (H95Q, H95N), but insensitive to mutations at K12. Binding of DHAP to wild-type yeast TIM results in a shift of the carbonyl stretching frequency from 1732 cm^{-1} in the free ligand to 1713 cm^{-1} in the bound state. In contrast, the observed stretching frequencies in the H95Q and H95N mutants (from 1732 to 1742 cm^{-1}) were unchanged, suggesting that the ε-ammonium group of Lys12 does not substantially contribute to polarization of the carbonyl group of DHAP.[11] Inspection of the yeast TIM/DHAP complex structure (PDB ID: 1NEY)[15] reveals that H95 is geometrically better positioned than the Lys12 ε-amino group to form a hydrogen bond to the carbonyl oxygen of DHAP [N(H95)–O dist: 2.72 Å, ∢CON(H95): 121.2°; N(K12)–O: 3.07 Å, ∢CON(K12): 105.3°]. The geometry

of approach is more favourable in the former case. However, the ε-amino group can contribute very substantially to the stabilization of the endiolate anion both electrostatically and through hydrogen bonding, because of rehybridization of the oxygen atom in the endiolate. Ionic hydrogen bonds are also substantially stronger than the interactions between neutral donors and acceptors.[35] Interestingly, the H95Q mutant showed a 500-fold reduction in enzyme activity, leading to the suggestion that an alternative mechanism of proton transfer is operative in the mutant.[11]

In this study, a 4000-fold loss of activity and a large conformational change of the K12 side chain has been established for the E97Q mutant of *Pf* TIM. It would therefore appear reasonable to assume a critical role for the fully conserved E97 residue in the catalytic process. Are the K12 and the E97 residues functioning only in precisely orienting the anionic substrate and the catalytically important H95 residue? The E97 side chain forms a strong hydrogen bond to the K12 ε-amino group (N–O, 2.8 Å). The planar carboxylic acid of E97 and the imidazole group of H95 are aligned approximately parallel and are close-packed, with an interplanar distance of ≈3.4 Å. Knowles and co-workers have pointed out that the neutral group of imidazole of H95 forms a hydrogen bond (=N···H–N 3.04 Å) with the backbone NH of E97. This would orient the imidazole such that the protonated nitrogen would be proximal to the substrate, and led to the proposal of a step involving proton abstraction from the neutral imidazole.[21]

At this juncture, the following question may be raised. Can the protonated ammonium group of K12 serve to transfer a proton to the oxygen atom at the C2 position of the enediolate anion, leading to the neutral enediol? Bash et al. noted in 1991 that although the pK_a of the enediol has not been measured, the values for enols are in the neighbourhood of 11.[19] The pK_a of the Lys ε-ammonium group might be slightly lower, so this transfer could indeed be favourable. In contrast, the pK_a for the process $His \rightarrow His^- + H^+$ is of the order of 14. His95 in its neutral form would then serve to abstract the proton from the C1 OH group of the neutral enediol, with subsequent ketonization and protonation of the C2 carbon by E165. Rapid proton transfer through the hydrogen bond network involving H95, E97 and K12 would restore the initial protonation states of these residues, thereby completing the catalytic cycle. In particular, a 180° flip of the His95 side chain about the Cβ–Cγ bond can transiently change the positions of the protonated and deprotonated N atoms, facilitating proton abstraction from the enediol and also proton transfer to re-establish charge states after the catalytic step. Indeed, a reaction-driven imidazole ring flip has been proposed at the active site of a serine protease.[36] Knowles did in fact anticipate "the seductive possibility… that the proton transfers are mediated merely by rotation of the appropriate side chain: the bidentate carboxyl group for the manipulation of carbon-bound protons, and the bidentate imidazole group for handling the oxygen-bound protons".[9] In the mechanism, proposed on the basis of the results presented here, summarized in Scheme 1, His95 is neutral

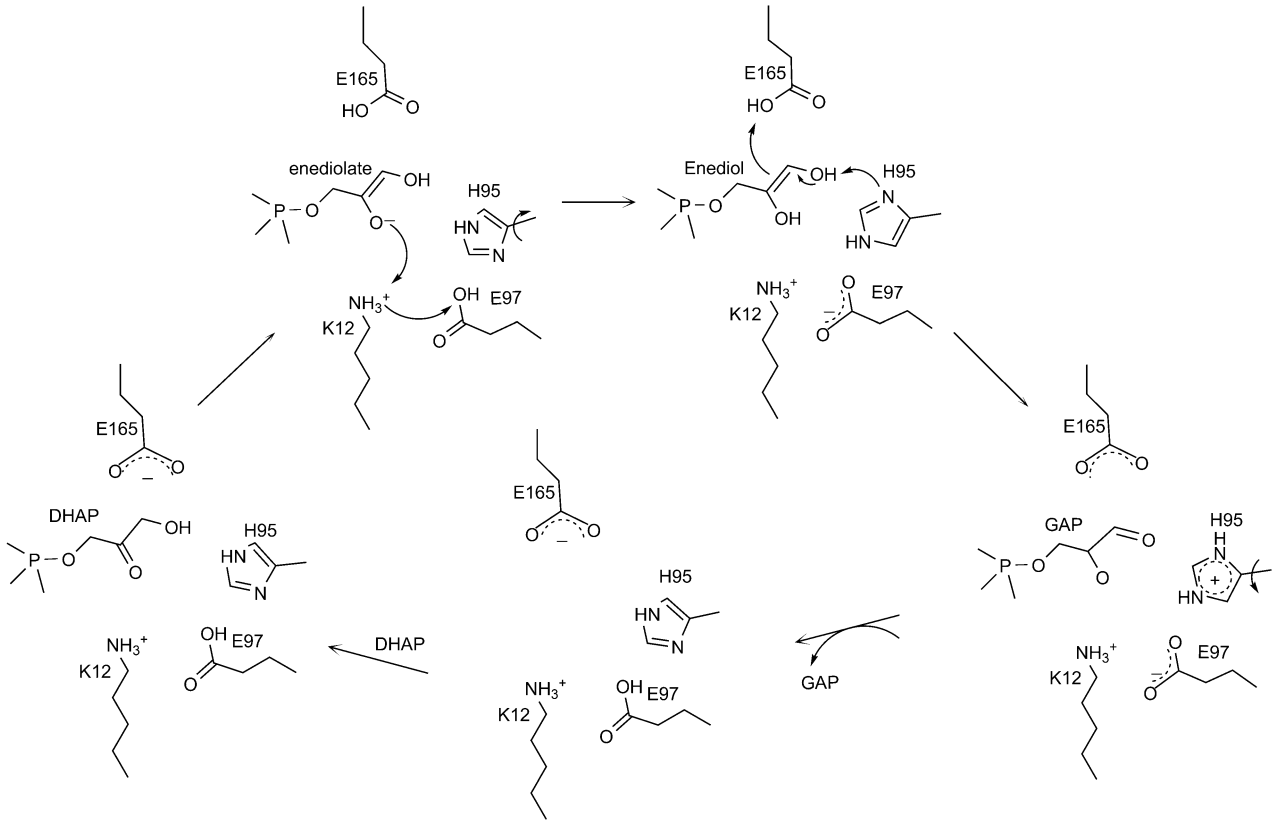

Scheme 1. Schematic representation of the proposed proton-transfer mechanism in the triosephosphate isomerase catalytic cycle.

in the resting state of the enzyme, as established by Knowles and co-workers. The candidate "electrophile" in this alternative mechanistic proposal, however, is the ε-ammonium group of K12, the Brönsted acidity of which might be more evenly matched with the basicity of the initially formed enediolate anion. His95 performs a critical—albeit more conventional—catalytic role in acting as a base for proton abstraction from the enediol. Bash et al. (1991) implicitly acknowledged the possibility of dynamic effects in noting: "Neither the structural data, nor the calculations can exclude the possibility that the transiently formed protonated His95 is the catalytic acid, nor that a concerted proton transfer between substrate oxygen atoms occurs via a neutral histidine as a relay".[19] In a comprehensive discussion of the role of Lys12 in the isomerization reaction catalysed by TIM, Richard and co-workers raised the issue of whether the intermediate is a charged enediolate or a neutral enediol. They suggest "that there is a strong catalytic imperative to the avoidance of full transfer of a proton to the enediolate oxyanion". They argue that "full proton transfer to the enediolate oxyanion could eliminate the large stabilizing electrostatic interaction with the cationic side chain of Lys12",[13] which undoubtedly is a critical interaction for the catalytic process. The alternative mechanistic proposal considered by us for the now classical isomerization reaction catalysed by triosephosphate isomerase is based on the finding that the E97Q mutant is 4000 times less active than the wild-type enzyme. This may be compared with the 500-fold loss of activity of the H95Q mutant.[11] The only striking structural difference between the wild-type enzyme and the E97Q mutant is the dramatic reorientation of the K12 side chain. Indeed, out of all the reported TIM structures, this is a sole example of a large change in the position of the K12 side chain. Conservation of the E97 residue in all TIM sequences so far reported suggests a critical role. The TIM active site is intricately constructed through the involvement of highly directional hydrogen-bonding interactions between the subunits, ensuring that dimerization is a prerequisite for optimal catalytic competence. The well-characterized monomeric TIMs engineered by Wierenga and co-workers are at least 1000 times less active than their dimeric counterparts.[23] Careful examination of the intersubunit interactions involving Glu(E) and Gln(Q) at position 97 led to the conclusion that this mutation leaves the dimer interface unperturbed. Indeed, experimental studies revealed no differences in the concentration dependence of biophysical parameters of the wild-type and mutant enzymes. These observations support the direct involvement of E97 in the catalytic cycle.

In the E97D mutant, the acidic group has been retained, but the side chain is significantly shortened. This mutant shows a significantly lower catalytic activity, with a reduction in k_{cat} of $\approx$100-fold. This observation is in contrast to that reported for the E97D mutant of the chicken enzyme,[22] which shows no loss of activity upon mutation. The reason for the differences between these earlier studies and our present report are not clear. Careful examination of the sequences and the crystal structures of the chicken (PDB ID: 1TPH) and *Pf* enzymes (PDB ID: 1O5X) establishes almost complete conservation of residues implicated in substrate binding and catalysis. Indeed the facile mutational interconversion of the codons for the E and D residues by changes at the third position (E: GAA, GAG; D: GAU, GAC) suggests that conservation must be driven by a strong phenotypic selection process. Inspection of the crystal structure of the E97D mutant reveals that the dimer interface interactions are maintained and the orientations of the carboxylate group of D97 and the imidazole group of H95 are also closely similar to those in the wild-type enzyme (Figures 4 and 5). The K12 side chain maintains the same position as in the wild-type enzyme, despite the absence of a hydrogen-bonding interaction with the carboxylate of D97. The corresponding N–O distances in the E97D structures are 4.83 Å and 4.47 Å. The fall in activity might therefore arise from a disruption of the hydrogen bond network involving residues K12, E97 and H95.

In all of the TIM sequences reported so far, multiple sequence alignment reveals only nine completely conserved residues, of which four are capable of accepting and donating protons. These four residues—two acidic (E165 and E97) and two basic (H95 and K12) residues—are arrayed around the small polar substrate. Whereas critical roles have been proposed for three of these residues—E165, H95 and K12—in binding and catalysis, no direct involvement of the conserved E97 residue has been suggested. The results of this study establish that the isosteric E97Q replacement results in a dramatic loss of catalytic activity and a large structural change in the critical K12 side chain. Shortening of the side chain at position 97, with retention of the acidic functionality in the E97D mutant, leads to a 100-fold drop in catalytic efficiency, despite the retention of the K12 side chain conformation identical to that observed in the wild-type TIM. We believe that these results provide compelling evidence of direct involvement of the E97 side chain in the proton-transfer reaction. The mechanistic proposal advanced by us eliminates the need to invoke the intermediacy of a chemically unlikely species, the imidazolate anion at H95.

Conclusions

In summary (Scheme 1), the proton-transfer cycle in the TIM-catalysed isomerization reaction begins with proton abstraction by the carboxylate anion of E165. A hydrogen bond network involving the enediolate anion, the ε-ammonium group of K12, the carboxylic acid of E97 and the neutral imidazole of H95 might provide a facile channel for proton hopping during the catalytic cycle. K12 might indeed play a critical role by abstracting a proton from the neutral E97 carboxylic acid, even as it loses a proton to the enediolate oxygen to yield a neutral enediol. It is conceivable that this concerted proton transfer occurs via a five-coordinate transition state at the ε-amino group of Lys12, thereby avoiding the need for full proton transfer to form a neutral amino group. Although the existence of pentacoordinate nitrogen species has been the subject of both experimental and theoretical debate, Olah and co-workers have suggested that this possibility may be considered for hydrogen because of its small covalent radius.[37] H95 can now act in a more conventional role as a base, abstracting the proton from the OH group on C1, setting in motion the re-

arrangement leading to reprotonation at C2 by transfer of the proton from the neutral E165 residue. Although dissection of the individual steps of proton transfer is useful in following through the states of protonation of acidic and basic residues during the catalytic cycles, it must be emphasised that all steps—proton transfer and side-chain flips—could occur in a near concerted manner. Although the resting state of the enzyme has been assumed to have a protonated (uncharged) E97 residue, it is conceivable that the anionic, ionized form might also mediate proton transfer between a transient imidazolium ion at H95 and a neutral ε-amino group at K12. Hydrogen-bond networks, when coupled to dynamic motions of catalytic residues, can indeed contribute to the high efficiency of enzymes involved in hydrogen-transfer reactions.[38] All the fully conserved residues in triosephosphate isomerase occur directly at the active site or in close proximity. Three attributes of triosephosphate isomerase, and indeed multimeric enzymes in general, are considered important for function. These are 1) proper folding into a native three-dimensional structure, 2) specific subunit association to give functional multimers, and 3) precise orientation of the active-site residues together with suitable conformational flexibility to accommodate the dynamic requirements of catalysis.[39] The availability of a large sequence dataset for enzymes suggests that there are multiple solutions to the problems of protein folding and specific protein–protein interactions leading to oligomerization. Catalytic chemistry is, however, more severely constrained, resulting in the overwhelming preponderance of fully conserved residues at the active site. This view echoes a four-decade-old paper by John Maynard Smith[40] that suggests, as paraphrased by Knowles, that "enzymes represent the rare end products of an extensive search through protein sequence space".[2]

Experimental Section

Mutagenesis: The *Plasmodium falciparum* triosephosphate isomerase gene was cloned into the expression vector pTrc99A, called pARC1008.[41] The protein was overexpressed into AA200, an ampicillin-resistant *E. coli* strain, from which the host TIM gene has been deleted.[42] To probe the role of the residue at 97, two single mutants—E97Q and E97D—were constructed by site-directed mutagenesis by the single-primer method.[43]

Because of the lack of availability of a restriction site at the desired position of mutation, a two-step process was followed:

Step 1) Generating the E97 int clone with the introduction of the restriction site of ECoRV at the desired position of mutation: In this step, the wild-type gene was taken as the template and the single 5′ primer 5′-GTTATT ATTGGT CATTTT **GATATC** AGAAAA TATTTC CATGAA ACCG-3′ was used with the ECoRV restriction site, to generate the E97 int clone.

Step 2: The intermediate clone was taken as the template and the mutant clones E97Q and E97D were generated with the subsequent removal of the restriction site of ECoRV and introduction of the required mutations. The 5′ primers used for generating the E97Q and E97D clones from the template E97 int clone were 5′-GTTATT ATTGGT CATTTT **CAG**AGA AGAAAA TATTTC CATGAA ACCG-3′ and 5′-GTTATT ATTGGT CATTTT **GAT**AGA AGAAAA TATTTC CATGAA ACCG-3′, respectively. For this study, another mutant, the E165A mutant, was also generated as an enzyme activity control in which the key catalytic base was replaced by alanine. For construction of this mutant the wild-type gene was used as the template and the single mutagenic 5′ primer 5′-GATAAT GTTATT TTGGCA TAT**GCA** CCTTTA TGGGCT ATTGGT AC-3′ was used with the restriction site NdeI (detailed protocols provided in the Supporting Information).

Protein expression and purification: *E. coli* AA200 cells (with deleted inherent TIM gene), transformed with the recombinant vector containing the mutant TIM gene, was grown at 37 °C in Terrific broth containing ampicillin (100 μg mL^{-1}). Cells were induced by use of IPTG (isopropyl-β-D-thiogalactopyranoside, 300 μM) at 0.6–0.8 $OD_{600\,nm}$ and were harvested by centrifugation. Cells were resuspended in lysis buffer [TrisHCl (pH 8.0, 20 mM), ethylenediaminetetraacetate (EDTA, 1 mM), phenylmethanesulfonylfluoride (PMSF, 0.01 mM), dithiothreitol (DTT, 2 mM) and glycerol (10%)] and disrupted by sonication. After centrifugation and removal of the cell debris, the supernatant was subjected to ammonium sulfate precipitation. The protein fraction containing TIM was selectively precipitated above 70% ammonium sulfate saturation. This precipitate was collected by centrifugation and resuspended in buffer A [TrisHCl (pH 8.0, 20 mM), DTT (2 mM) and glycerol (10%)]. Removal of nucleic acid was effected by polyethylene imine precipitation. All purification steps were carried out at 4 °C. The protein was dialysed extensively against buffer A at 4 °C overnight, purified with the aid of an anion-exchange column (Q-sepharose, HR 60) and eluted with a linear gradient of NaCl (0–1 M). The fractions containing the protein were pooled and precipitated by addition of ammonium sulfate up to a concentration of 75%. The precipitated protein was dissolved in buffer A and subjected to gel filtration chromatography (Sephacryl-200), with equilibration with the same buffer in an AKTA BASIC FPLC system. Protein purity was checked by 12% SDS-PAGE. The masses of the mutant proteins were confirmed by LC ESI MS with an ion trap mass spectrometer or a Q TOF system. Protein concentration was determined by Bradford's method[44] with use of BSA as a standard. Protein yields of 40–50 mg L^{-1} of *E. coli* culture was obtained.

Enzyme assay: Kinetic measurements were carried out by the method of Plaut and Knowles[45] at room temperature. The TIM-promoted conversion of GAP (glyceraldehyde 3-phosphate) into DHAP (dihydroxyacetone phosphate) was coupled to the subsequent reaction by use of the coupling enzyme α-glycerol phosphate dehydrogenase. In this coupled assay reaction, a total reaction volume of 1 mL contained TEA (pH 7.6, 100 mM), EDTA (5 mM), NADH (0.5 mM), α-glycerol phosphate dehydrogenase (20 μg mL^{-1}) and GAP, to which TIM was added at the end. Whereas in the case of the wild-type enzyme the assay could be started with 10 ng of the protein, in the cases of the mutants, 1000 ng of E97D, 10000 ng of E97Q and 10000 ng of E165A were needed to initialize the reaction. Substrate concentrations were varied from 0.25 mM to 4.0 mM. The enzyme activity was determined by monitoring the decrease in absorbance of NADH at 340 nm. The extinction coefficient of NADH was taken to be 6220 M^{-1} cm^{-1} at 340 nm.[46] The experiments were repeated at least three times from independent purification batches. The values for the kinetic parameters (K_m, k_{cat}) were determined by fitting to Michaelis–Menten equation with the aid of Graphpad Prism software (Version 5 for Windows, Graphpad Software, San Diego, California, USA, http://www.graphpad.com).

Fluorescence spectroscopy, circular dichroism and size-exclusion chromatography: Experimental details are provided in the Supporting Information.

Table 2. X-ray diffraction data collection statistics.

	E97Q	E97D
PDB ID	3PSW	3PSV
space group	$P2_122_1$	$P2_122_1$
unit cell *a* [Å]	50.91	51.06
b [Å]	53.75	53.77
c [Å]	174.48	174.70
$\alpha=\beta=\gamma$ [°]	90	90
resolution range [Å]	45.80–1.99	43.70–2.00
no. of reflections	217608	286503
no. of unique reflections	33609	33483
completion [%][b]	90.20 (93.80)	95.40 (95.30)
overall *R* merge[%][b]	19.80 (53.50)	12.10 (43.00)
multiplicity[b]	7.20 (5.00)	9.0 (8.0)
$\langle I/\sigma I\rangle$[b]	15.23 (2.88)	28.28 (5.84)
average mosaicity	0.30	0.30

[b] Represents highest-resolution shells.

Table 3. Crystallographic refinement statistics.

	E97Q	E97D
resolution range [Å]	45.8–1.99	43.7–2.0
number of subunits/asymmetric unit	2	2
number of reflections used	30019	31746
% observed	89.3	94.9
R_{work} [%]	20.1	18.5
R_{free} [%]	25	23
Model quality		
number of protein atoms	4358	4341
number of water molecules	475	456
average *B* factor [Å^2]: protein	20.43	18.44
water	31.45	29.56
RMSD from ideal: bond length [Å]	0.007	0.007
bond angle [°]	0.96	0.98
Ramachandran statistics		
most-allowed region [%]	93.8	93.6
allowed region [%]	6.2	6.4
generously allowed region [%]	0	0
disallowed region [%]	0	0

Crystallization of E97Q and E97D: A protein concentration of 10 mg mL^{-1} was used for crystallization experiments based on the hanging drop method, in which each crystallization droplet contained protein ($\approx$10 mg mL^{-1}, 3 μL) with cocktail buffer (3 μL) and was equilibrated with reservoir solution (500 μL). The E97Q crystal used for data collection was obtained under these conditions: PEG (24%), HEPES buffer (pH 7.0, 100 mM), DTT (0.5 mM), sodium azide (0.5 mM) and Li_2SO_4 (10 mM). The E97D crystal was obtained under these conditions: PEG (16%), HEPES buffer (pH 7.0, 100 mM, DTT (0.5 mM), sodium azide (0.5 mM) and Li_2SO_4 (10 mM).

Data collection and processing: The crystals were transferred into crystallization buffer containing ethylene glycol (20%) as cryoprotectant, before mounting on the cryoloop. X-ray diffraction data were collected with a Rigaku rotating anode generator and a MAR Research image plate detector system. The data sets were indexed, integrated and scaled with the aid of DENZO and SCALEPACK from the HKL2000 suite of programs.[47] Table 2 summarizes the crystallographic parameters and the data collection statistics.

Structure solution and refinement: The structures of E97Q and E97D were solved by use of the molecular replacement program PHASER from the CCP4 package.[48] The native *Pf* TIM crystal structure (PDB ID: 1O5X) was used as the starting model. The coordinates of 1O5X were modified by removal of the loop 6 residues, ligand, water molecules and alternate conformations. Refinement of both structures was carried out by use of REFMAC,[49] with 20 initial cycles of rigid body refinement followed by 50 cycles of restrained refinement. Loop 6 residues, ligand and water molecules were subsequently added into the electron density maps, $|2F_o-F_c|$ and $|F_o-F_c|$ contoured at 1σ and 3σ respectively. The model building was done with use of COOT.[50] In both structures, two subunits were observed in the asymmetric unit. The existence of the E97Q and E97D mutations was confirmed from the difference Fourier maps. Water molecules were first located automatically by COOT and validated if a peak was observed above 3σ on a difference map and 1.5σ on a double difference map. Both structures were refined to reasonable R_{work} and R_{free} values. The geometries of the final structures were examined with the aid of the PROCHECK program[51] in the CCP4 package. The refinement statistics for the structures are summarized in Table 3.

Acknowledgements

P.B. is deeply indebted to N. V. Joshi for his analysis of TIM sequences and helpful discussions. We thank Kallol Gupta for the mass spectral analysis of the mutant proteins. M.S. was supported by a Senior Research Fellowship from the Council of Scientific and Industrial Research (India). Research on TIM was supported under a grant from the Department of Science and Technology (India). X-ray diffraction and mass spectrometry facilities were supported by program grants from the Department of Science and Technology and Department of Biotechnology (India).

Keywords: active sites · enzyme mechanisms · isomerases · mutagenesis · proton transfer

[1] M. Karplus, J. Kuriyan, *Proc. Natl. Acad. Sci. USA* **2005**, *102*, 6679–6685.
[2] J. R. Knowles, *Phil. Trans. R. Soc. Lond. B* **1991**, *332*, 115–121.
[3] R. K. Wierenga, E. G. Kapetaniou, R. Venkatesan, *Cell. Mol. Life Sci.* **2010**, *67*, 3961–3982.
[4] S. C. Blacklow, R. T. Raines, W. A. Lim, P. D. Zamore, J. R. Knowles, *Biochemistry* **1988**, *27*, 1158–1167.
[5] S. V. Rieder, I. A. Rose, *J. Biol. Chem.* **1959**, *234*, 1007–1010.
[6] W. J. Albery, J. R. Knowles, *Biochemistry* **1976**, *15*, 5627–5631.
[7] W. J. Albery, J. R. Knowles, *Biochemistry* **1976**, *15*, 5621–5626.
[8] W. J. Albery, J. R. Knowles, *Biochemistry* **1976**, *15*, 5631–5640.
[9] J. R. Knowles, *Nature* **1991**, *350*, 121–124.
[10] R. T. Raines, E. L. Sutton, D. R. Straus, W. Gilbert, J. R. Knowles, *Biochemistry* **1986**, *25*, 7142–7154.
[11] E. A. Komives, L. C. Chang, E. Lolis, R. F. Tilton, G. A. Petsko, J. R. Knowles, *Biochemistry* **1991**, *30*, 3011–3019.
[12] P. J. Lodi, L. C. Chang, J. R. Knowles, E. A. Komives, *Biochemistry* **1994**, *33*, 2809–2814.
[13] M. K. Go, A. Koudelka, T. L. Amyes, J. P. Richard, *Biochemistry* **2010**, *49*, 5377–5389.
[14] M. Alahuhta, R. K. Wierenga, *Proteins Struct. Funct. Bioinf.* **2010**, *78*, 1878–1888.
[15] G. Jogl, S. Rozovsky, A. E. McDermott, L. Tong, *Proc. Natl. Acad. Sci. USA* **2003**, *100*, 50–55.
[16] L. Pauling, *The Nature of the Chemical Bond*, 3rd ed., Cornell University Press, New York, **1960**.
[17] T. L. Amyes, A. C. O'Donoghue, J. P. Richard, *J. Am. Chem. Soc.* **2001**, *123*, 11325–11326.

[18] J. R. Morrow, T. L. Amyes, J. P. Richard, *Acc. Chem. Res.* **2008**, *41*, 539 – 548.
[19] P. A. Bash, M. J. Field, R. C. Davenport, G. A. Petsko, D. Ringe, M. Karplus, *Biochemistry* **1991**, *30*, 5826 – 5832.
[20] M. K. Go, A. Koudelka, J. P. Richard, *J. Am. Chem. Soc.* **2010**, *132*, 13525 – 13532.
[21] P. J. Lodi, J. R. Knowles, *Biochemistry* **1991**, *30*, 6948 – 6956.
[22] S. C. Blacklow, K. D. Liu, J. R. Knowles, *Biochemistry* **1991**, *30*, 8470 – 8476.
[23] a) T. V. Borchert, R. Abagyan, R. Jaenicke, R. K. Wierenga, *Proc. Natl. Acad. Sci. USA* **1994**, *91*, 1515 – 1518; b) T. V. Borchert, J. P. Zeelen, W. Schliebs, M. Callens, W. Minke, R. Jaenicke, R. K. Wierenga, *FEBS Lett.* **1995**, *367*, 315 – 318; c) M. Salin, E. G. Kapetaniou, M. Vaismaa, M. Lajunen, M. G. Casteleijn, P. Neubauer, L. Salmon, R. K. Wierenga, *Acta Crystallogr. Sect. D Biol. Crystallogr.* **2010**, *66*, 934 – 944.
[24] P. Pattanaik, G. Ravindra, C. Sengupta, K. Maithal, P. Balaram, H. Balaram, *Eur. J. Biochem.* **2003**, *270*, 745 – 756.
[25] S. S. Velanker, S. S. Ray, R. S. Gokhale, S. Suma, H. Balaram, P. Balaram, M. R. N. Murthy, *Structure* **1997**, *5*, 751 – 761.
[26] P. Gayathri, M. Banerjee, A. Vijayalakshmi, S. Azeez, H. Balaram, P. Balaram, M. R. N. Murthy, *Acta Crystallogr. Sect. D Biol. Crystallogr.* **2007**, *63*, 206 – 220.
[27] H. Walden, G. S. Bell, R. J. Russell, B. Siebers, R. Hensel, G. L. Taylor, *J. Mol. Biol.* **2001**, *306*, 745 – 757.
[28] S. C. Lovell, J. M. Word, J. S. Richardson, D. C. Richardson, *Proc. Natl. Acad. Sci. USA* **1999**, *96*, 400 – 405.
[29] I. Rose, *Autobiography, The Nobel Prize in Chemistry*, http://www.nobelprize.org **2004**.
[30] a) E. Lolis, G. A. Petsko, *Biochemistry* **1990**, *29*, 6619 – 6625; b) R. C. Davenport, P. A. Bash, B. A. Seaton, M. Karplus, G. A. Petsko, D. Ringe, *Biochemistry* **1991**, *30*, 5821 – 5826; c) Z. Zhang, S. Sugio, E. A. Komives, K. D. Liu, J. R. Knowles, G. A. Petsko, D. Ringe, *Biochemistry* **1994**, *33*, 2830 – 2837.
[31] a) N. S. Sampson, J. R. Knowles, *Biochemistry* **1992**, *31*, 8482 – 8487; b) J. C. Williams, A. E. McDermott, *Biochemistry* **1995**, *34*, 8309 – 8319; c) Y. Wang, R. B. Berlow, J. P. Loria, *Biochemistry* **2009**, *48*, 4548 – 4556.
[32] M. M. Malabanan, T. L. Amyes, J. P. Richard, *Curr. Opin. Struct. Biol.* **2010**, *20*, 702 – 710.
[33] P. J. Lodi, J. R. Knowles, *Biochemistry* **1993**, *32*, 4338 – 4343.
[34] Q. Cui, M. Karplus, *J. Am. Chem. Soc.* **2002**, *124*, 3093 – 3124.
[35] M. Meot-Ner, *Chem. Rev.* **2005**, *105*, 213 – 284.
[36] E. L. Ash, J. L. Sudmeier, R. M. Day, M. Vincent, E. V. Torchilin, K. C. Haddad, E. M. Bradshaw, D. G. Sanford, W. W. Bachovchin, *Proc. Natl. Acad. Sci. USA* **2000**, *97*, 10371 – 10376.
[37] K. O. Christe, W. W. Wilson, G. J. Schrobilgen, R. V. Chirakal, G. A. Olah, *Inorg. Chem.* **1988**, *27*, 789 – 790.
[38] J. P. Klinman, *Chem. Phys. Lett.* **2009**, *471*, 179 – 193.
[39] a) Z. D. Nagel, J. P. Klinman, *Nat. Chem. Biol.* **2009**, *5*, 543 – 550; b) S. D. Schwartz, V. L. Schramm, *Nat. Chem. Biol.* **2009**, *5*, 551 – 558.
[40] J. Maynard Smith, *Nature* **1970**, *225*, 563 – 564.
[41] J. Ranie, V. P. Kumar, H. Balaram, *Mol. Biochem. Parasitol.* **1993**, *61*, 159 – 169.
[42] A. Anderson, R. A. Cooper, *J. Gen. Microbiol.* **1970**, *62*, 329 – 334.
[43] A. R. Shenoy, S. S. Visweswariah, *Anal. Biochem.* **2003**, *319*, 335 – 336.
[44] M. M. Bradford, *Anal. Biochem.* **1976**, *72*, 248 – 254.
[45] B. Plaut, J. R. Knowles, *Biochem. J.* **1972**, *129*, 311 – 320.
[46] B. L. Horecker, A. Kornberg, *J. Biol. Chem.* **1948**, *175*, 385 – 390.
[47] Z. Otwinowski, W. Minor, *Methods Enzymol.* **1997**, *276*, 307 – 326.
[48] A. J. McCoy, R. W. Grosse-Kunstleve, P. D. Adams, M. D. Winn, L. C. Storoni, R. J. Read, *J. Appl. Crystallogr.* **2007**, *40*, 658 – 674.
[49] G. N. Murshudov, A. A. Vagin, E. J. Dodson, *Acta Crystallogr. Sect. D Biol. Crystallogr.* **1997**, *53*, 240 – 255.
[50] P. Emsley, K. Cowtan, *Acta Crystallogr. Sect. D Biol. Crystallogr.* **2004**, *60*, 2126 – 2132.
[51] R. A. Laskowski, M. W. MacArthur, D. S. Moss, J. M. Thornton, *J. Appl. Crystallogr.* **1993**, *26*, 283 – 291.

Received: February 16, 2011
Published online on June 10, 2011

